Fracture Mechanics of Concrete and Concrete Structures -
Recent Advances in Fracture Mechanics of Concrete - B. H. Oh, et al.(eds)

A comparative study between smeared and embedded crack models for finite element analysis of reinforced concrete beams

A.L. Gamino & J.L.A.O. Sousa
University of Campinas, Campinas, Brazil

O.L. Manzoli
São Paulo State University, Bauru, Brazil

T.N. Bittencourt
University of São Paulo, São Paulo, Brazil

ABSTRACT: The nonlinear behavior of concrete when loaded monotonically through a quasi-static loading process is associated to the nucleation and growth of micro-pores and micro-cracks in small regions. This localized degradation of the mechanical properties culminates in material failure in form of strong discontinuity (discontinuity of the displacement field) or crack. One of the greatest efforts of the last decades in the field of the computational mechanics corresponds to the development of efficient and robust strategies to simulate discontinuities formation and propagation using the Finite Element Method. In the smeared crack models, the strong discontinuity associated to the crack is spread throughout the finite element. As well known, the continuity of the displacement field assumed for these models is not compatible with the real discontinuity. Despite this, this type of models has been extensively used due to its relative computational simplicity provided by treating cracks using a continuum framework, as well as due to the reported good predictions of the structural behavior of reinforced concrete members. On the other hand, the embedded crack model is able to describe the effects of real discontinuities (cracks), by enriching the displacement field in the interior of each finite element crossed by the crack paths. This paper presents a comparative study between the abilities of these two models to predict the mechanical behavior of reinforced concrete beams. Structural responses, crack patterns, rebars and concrete stresses, predicted by both models are compared with experimental results from literature.

1 INTRODUCTION

In the evolution of the nonlinear analysis of reinforced concrete structures using the Finite Element Method (FEM), the Scordelis' pioneer work in the 1960's defined concepts and criteria to be followed by the research community in this area. From the many contributions of Prof. Scordelis, this paper addresses the classic laboratory tests of twelve reinforced concrete beams (Bresler & Scordelis 1963) developed with the objective of investigating the critical shear behavior of the beams and also producing experimental results to support numerical developments in finite elements. These beam tests were considered as a classic series by the scientific community. Since then, these results were used intensively as reference data for calibration and verification of numerical models for reinforced concrete structures using the FEM.

Recently, in 2004 (Vecchio & Shim 2004), another experimental program developed in the University of Toronto, in Canada, reproduced the classic tests of RC beams, tracking the post-peak behavior by means of force-displacement curves. This paper describes the numerical modeling of those beams using smeared crack model and embedded crack model. Another significant contribution for the crack modeling was accomplished by (Ngo & Scordelis 1967). Although simple model, it represents a step ahead in the field of computational development for the simulation of cracks in concrete structures.

In a previous paper (Gamino & Bittencourt 2007) the authors reported a FEM simulations of numerical evaluation of plastic rotation capacity in R/C beams using commercials codes and an implementation of a smeared rotating crack model. This paper presents a comparative study between the abilities of a smeared rotating crack model and an embedded crack model to predict the mechanical behavior of reinforced concrete structures.

2 SMEARED CRACK MODEL

Coupled with the model of physical integrity, a model of rotating smeared crack was implemented. The cracking criterion compares the tensile stresses (from Ottosen's model 1977) in the Gauss points with the material tensile strength. After the onset of the first crack, a linear softening model was used (Figure 1). More details can be seen in Gamino et al. (2007) and Gamino et al. (2009). Using a linear softening model in tension, the crack opening can be obtained through:

$$w^{cr} = \varepsilon^{cr} h \tag{1}$$

where: w^{cr} = crack width, ε^{cr} = crack strain and h = crack band width.

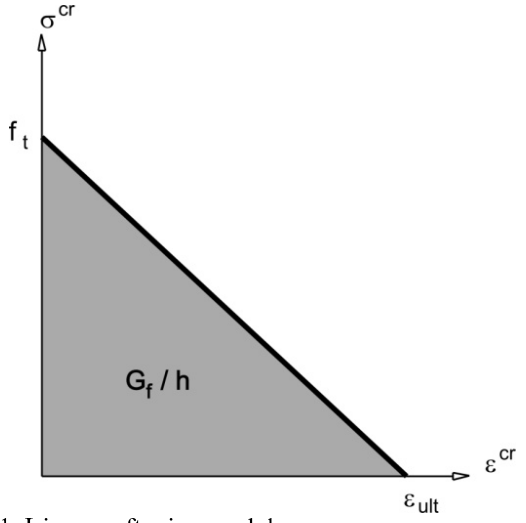

Figure 1. Linear softening model.

The crack opening displacements were computed from the crack strains, which depend on the failure models adopted for the concrete and the steel reinforcement. The used reinforcement ratios influence the stress level in the tensile portion of the structure, and thus the crack opening displacements. Therefore, crack opening displacements decrease as the reinforcement ratio increases. Crack opening displacements depend also on the tension-softening model adopted. The deformations in concrete can be obtained through:

$$\boldsymbol{\varepsilon} = \boldsymbol{\varepsilon}_e + \boldsymbol{\varepsilon}^{cr} \tag{2}$$

where: ε_e = elastic strain vector obtained from elastic matrix and $\boldsymbol{\varepsilon}^{cr}$ = crack strain vector obtained from the contribution of the concrete's degradation process.

The total strain vector $\boldsymbol{\varepsilon}$ in concrete can be obtained by:

$$\underbrace{\begin{Bmatrix}\varepsilon_x\\ \varepsilon_y\\ \gamma_{xy}\end{Bmatrix}}_{\boldsymbol{\varepsilon}} = \underbrace{\frac{\sigma}{E}\begin{Bmatrix}1\\ -\nu\\ 0\end{Bmatrix}}_{\boldsymbol{\varepsilon}_e} + \underbrace{\frac{w^{cr}}{2A}\begin{Bmatrix}y_1 - y_2\\ 0\\ x_2 - x_1\end{Bmatrix}}_{\boldsymbol{\varepsilon}^{cr}} \tag{3}$$

where A is the finite element area, x_i and y_i are the nodal coordinates.

The angle α in Figure 2 indicates the direction of the of the principal strain vector. Crack propagates in the perpendicularly to this direction (Jirásek & Zimmermann 1998):

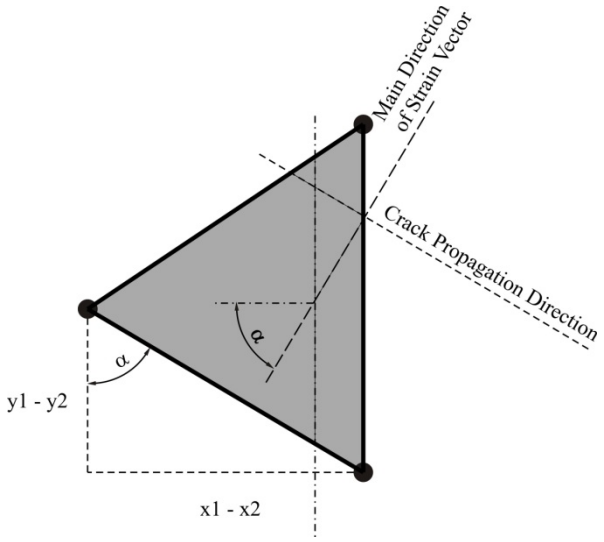

$$\alpha = \frac{1}{2} arctan \frac{\gamma_{xy}}{\varepsilon_x - \varepsilon_y} \tag{4}$$

Figure 2. Crack propagation direction.

3 EMBEDDED CRACK MODEL

In embedded representation the crack formation zone is modeled by introducing a very thin interface band into the finite element, whose behavior is described by a continuum damage constitutive model, in the context of the Continuum Strong Discontinuity Approach (CSDA), proposed by Oliver and collaborators (Oliver et al. 1999, Oliver 2000, Oliver et al. 2008, Manzoli & Shing 2006, Manzoli et al. 2008). The damage model criterion is based on the concrete tension strength, f_t and the softening law provides energy dissipation compatible with the concrete fracture energy, G_f.

Although dealing with a continuum constitutive stress-strain relation at the interface, it can be shown that this is equivalent to an approach using a discrete (cohesive) constitutive relation, involving displacement jumps and stresses (Oliver 2000).

Figure 3 illustrates a linear finite element with three nodes and two-dimensional domain Ω_e, crossed by a discontinuous interface S_e, that divides

the element in two parts isolating node 1 from the others.

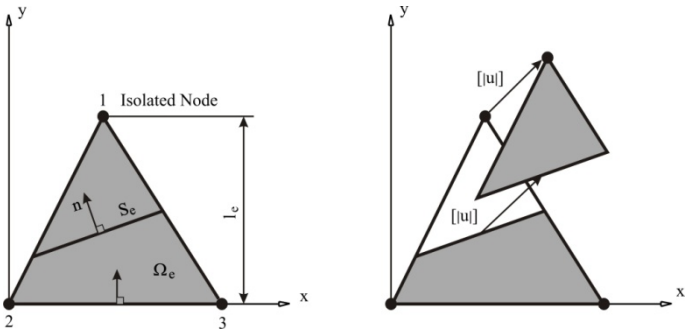

Figure 3. Finite element with embedded discontinuity.

A damage constitutive model has been used for the interface (Cervera et al. 1996). The unitary vectors $\mathbf{n}=\{n_x,\ n_y\}^T$ and $\mathbf{m}=\{m_x,\ m_y\}^T$ are normal to interface and to the isolated node opposing side, respectively, in accordance with the local system of cartesian reference (x, y) with the axis "x" parallel to the opposing side of the isolated node. More details can be found in (Manzoli & Shing 2006). The presence of the discontinuity provides a relative displacement of the isolated node:

$$\mathbf{d}_1 = \left[\left|\mathbf{u}\right|\right];\quad \mathbf{d}_2 = \mathbf{0};\quad \mathbf{d}_3 = \mathbf{0} \tag{5}$$

where $\left[\left|\mathbf{u}\right|\right]$ is the displacement discontinuity vector.

The nodal displacements produced by the discontinuity reflect the relative rigid-body motion between the two parts of the finite element. Therefore, when determining the strains $\boldsymbol{\varepsilon}=\{\varepsilon_x,\ \varepsilon_y,\ \gamma_{xy}\}^T$ from the element nodal displacements, the component of the nodal displacements associated to the discontinuity, $\mathbf{d}_i$, must be subtracted from the total displacements, $\mathbf{D}_i$:

$$\boldsymbol{\varepsilon} = \sum_{i=1}^{n} \mathbf{B}_i \left(\mathbf{D}_i - \mathbf{d}_i\right) = \sum_{i=1}^{n} \mathbf{B}_i \mathbf{D}_i - \mathbf{B}_i \left[\left|\mathbf{u}\right|\right] = \mathbf{B}\mathbf{D} - \boldsymbol{\varepsilon}^{cr} \tag{6}$$

where $\mathbf{B}$ is the standard finite element strain-displacement matrix.

The strain crack vector is given by:

$$\begin{Bmatrix} \varepsilon_x^{cr} \\ \varepsilon_y^{cr} \\ \gamma_{xy}^{cr} \end{Bmatrix} = \underbrace{\begin{bmatrix} m_x & 0 \\ 0 & m_y \\ m_y & m_x \end{bmatrix}}_{\mathbf{M}} \begin{Bmatrix} \left[\left|u\right|\right]_x \\ \left[\left|u\right|\right]_y \end{Bmatrix} = \frac{\mathbf{M}}{l_e}\left[\left|\mathbf{u}\right|\right] \tag{7}$$

where $\mathbf{M}$ is the matrix casting the components of the vector $\mathbf{m}$ and l_e is the distance between the isolated node and its opposite side (see Figure 3).

Finally, the explicit stiffness matrix of the element with incorporated discontinuity becomes:

$$\mathbf{K} = \left[\mathbf{B}^T\mathbf{C}\mathbf{B} - \mathbf{B}^T\mathbf{C}\frac{\mathbf{M}}{l_e}\left(\mathbf{N}^T\bar{\mathbf{C}}\left(\frac{\mathbf{M}}{l_e} - \frac{\mathbf{N}}{k}\right) - \mathbf{N}^T\bar{\mathbf{C}}\frac{\mathbf{M}}{l_e}\right)^{-1}\mathbf{N}^T\left(\bar{\mathbf{C}} - \mathbf{C}\right)\mathbf{B}\right]A \tag{8}$$

where $\bar{\mathbf{C}}$ is the interface tangent constitutive matrix, k is the interface bandwidth and

$$\mathbf{N}^T = \begin{bmatrix} n_x & 0 & n_y \\ 0 & n_y & n_x \end{bmatrix} \tag{9}$$

4 COMPUTATIONAL MODELING

The OA3 beam by Bresler & Scordelis (1963) shown in Figure 4 has been used to validate the implemented crack models.

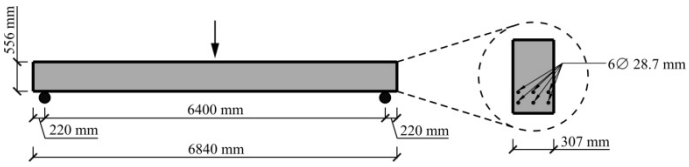

Figure 4. Test setup for OA3 beam tested by Bresler & Scordelis (1963).

The concrete and steel material properties used in the numerical simulations are:

- concrete: Young's modulus 22,300 MPa, Poisson ratio 0.15, compressive strength 37.6 MPa, tensile strength 3.0 MPa and fracture energy in mode-I 0.075N/mm.
- rebars: Young's modulus 218,000 MPa, Poisson ratio 0.30 and yield strength 555 MPa.

The Figure 5 shows the load-displacement curves, Figure 6 shows the load-axial strain curves (experimental and numerical) corresponding to the steel bottom reinforcement, Figure 7 shows the crack pattern and Figure 8 shows the crack width obtained from the implemented rotating smeared crack and embedded crack models.

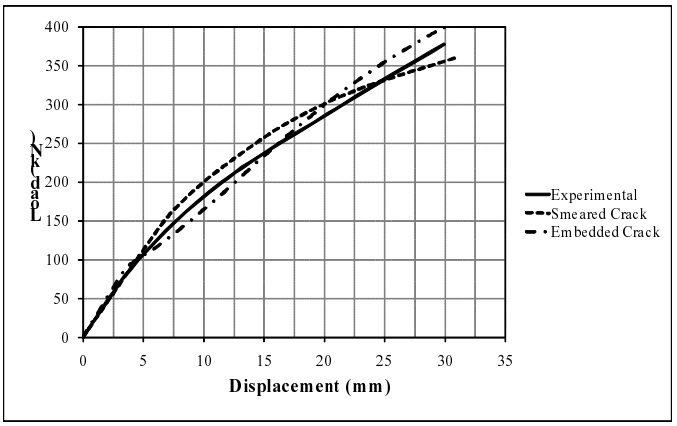

Figure 5. Load-displacement curves obtained for OA3 beam tested by Bresler & Scordelis (1963).

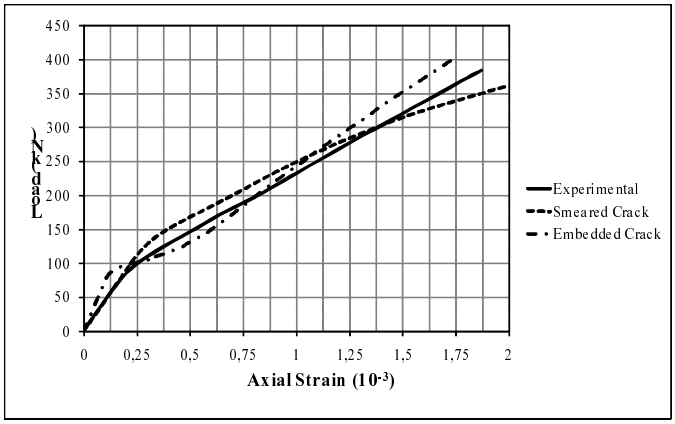

Figure 6. Load-strain curves to bottom reinforcement steel obtained for OA3 beam tested by Bresler & Scordelis (1963).

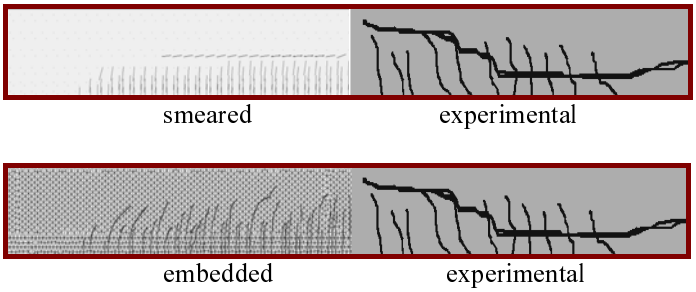

Figure 7. Crack patterns obtained for OA3 beam tested by Bresler & Scordelis (1963).

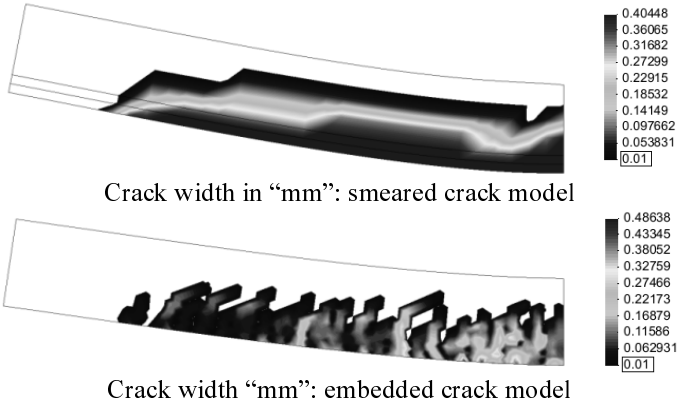

Figure 8. Numerical crack width obtained for OA3 beam tested by Bresler & Scordelis (1963).

Considering overall results, good correlation was obtained between the numerical response and experimental results from Bresler & Scordelis (1963) (displacements calculated with smeared or embedded crack models were particularly close to those from the experimental tests).

In experimental tests a maximum crack width 0.35 mm was obtained, while 0.30 mm was obtained using a smeared crack model and 0.48 mm using an embedded crack model. In a general manner the numerical results, in terms of crack opening, crack patterns, displacements and axial strain in bottom steel reinforcement, for the modeled beam were reasonable.

5 CONCLUSIONS

This work attempted to reproduce numerically a classic test of reinforced concrete beam in order to validate two formulations for the crack representation. The following conclusions can be drawn:

- In a general way, good correlation was obtained between the numerical response and the experimental observations of (Bresler & Scordelis 1963) for the OA3 beam (displacements calculated with smeared or embedded crack models were particularly close to those from the experimental tests);
- In experimental tests a maximum crack width 0.35 mm was obtained, while 0.30 mm was obtained using a smeared crack model and 0.48 mm using an embedded crack model;
- In a general manner the crack patterns and axial strain in bottom steel reinforcement for the modeled beam were reasonable.

REFERENCES

Bresler, B. & Scordelis, A.C. 1963. Shear strength of reinforced concrete beams. *Journal of American Concrete Institute*, 60(1): 51-74.

Gamino, A.L. & Bittencourt, T.N. 2007. Numerical evaluation of plastic rotation capacity in reinforced-concrete beams. In Alberto Carpinteri, Pietro Gambarova, Giuseppe Ferro & Giovanni Plizzari (ed.), *6th International Conference on Fracture Mechanics of Concrete and Concrete Structures; Catania, 17-22 Jun 2007*. London: Taylor & Francis.

Gamino, A.L., Bittencourt, T.N. & Sousa, J.L.A.O. 2007. Numerical Modeling of Classic Concrete Beam Tests. *IBRACON Structural Journal*, 3(2): 201-229.

Gamino, A.L., Bittencourt, T.N. & Sousa, J.L.A.O. 2009. Finite element computational modeling of externally bonded CFRP composites flexural behavior in RC beams. *Computers and Concrete – An International Journal*, 6(3): 187-202.

Manzoli, O.L. & Shing P.B. 2006. A general technique to embed non-uniform discontinuities into standard solid finite elements .*Computers & Structures*, 84(10-11): 742-757.

Manzoli, O. L., Oliver, J., Huespe, A. E. & Diaz, G. 2008. A mixture theory based method for three dimensional modeling of reinforced concrete members with embedded crack finite elements. *Computers & Concrete – An International Journal*, 5(4):401-416.

Ngo, D. & Scordelis, A.C. 1967. Finite element analysis of reinforced concrete beams. *ACI Journal*, 64(3): 152-163.

Oliver, J., Cervera, M. & Manzoli, O. 1999. Strong discontinuities and continuum plasticity models: the strong discontinuity approach. *International Journal of Plasticity*, 15:319-351.

Oliver, J., Linero, D., Huespe, A. & Manzoli, O.L. 2008. Two Dimensional Modeling of Material Failure in Reinforced Concrete by means of a Continuum Strong Discontinuity Approach. *Comput. Methods Appl. Mech. Eng*., 197:332-348.

Ottosen, N.S. 1977. A failure criterion for concrete. *Journal of the Engineering Mechanics Division*, 103(4): 527-535.

Vecchio, F.J. & Shim, W. 2004. Experimental and Analytical Re-examination of Classic Concrete Beam Tests. *ASCE Journal of Structural Engineering*, 130(3): 460-469.